Improving the efficiency of a GaInP solar cell using an AlGaAs buffer layer by optimizing the thicknesses of the PN junction

L. Djedoui[a], A. Aissat [a, c*], A. Djemouai[b], J. Vilcot[c]

[a]LATSI Laboratory, Department of electronics, Faculty of Technology, University of Saad Dahlab Blida1, Blida 09000, Algeria
[b]ETA Laboratory, Department of electronics, Faculty of technology, University Bordj Bou Arreridj, Bordj Bou Arreridj 34000, Algeria
[c]Institute of Electronics, Microelectronics and Nanotechnology (IEMN), UMR CNRS 8520, University of Sciences and Technologies of Lille 1, Avenue Poincare, 60069, 59652 Villeneuve of Ascq, France

In this work, the design and simulation of an GaInP single junction solar cell are presented. The work focuses mainly on the optimization of the PN junction thicknesses of n-base and p-emitter cell layers in order to improve the cell conversion efficiency. Besides this optimization, the layers of the cell window AlGaInP and an added buffer AlGaAs were also optimized in term of doping and thicknesses using Atlas tool of SILVACO TCAD. The cell is simulated under the conditions of 1 sun and AM1.5G solar spectrum at 25°C. The simulated GaInP solar cell demonstrates an efficiency (η) of 22.42%. The cell shows different electrical behaviors in terms of short circuit current density (J_{sc}), open circuit voltage (V_{oc}), fill factor (FF), and external quantum efficiency (EQE). The obtained results are compared with those reported in the literature. Simulation results of the cell are: a J_{sc} of 18.35 mA/cm^2, V_{oc} of 1.41 V and FF of 86.81% with the corresponding n-base layer and p-emitter layer thickness of 0.410 µm and 0.174 µm respectively and the total device thickness of 0.65 µm. According to these results, the proposed cell demonstrates an improvement in the efficiency and a reduction of the used GaInP material.

1. Introduction

Ternary $Ga_xIn_{1-x}P$, $Al_xGa_{1-x}As$ and quaternary $(Al_xGa_{1-x})_yIn_{1-y}P$ compound semiconductor materials are widely used in the area of optoelectronic devices. Particularly, $Ga_xIn_{1-x}P$ is a key material for the top cell in Multi-Junction Solar Cells [1]. Efficiency of GaInP and GaAs single junction and GaInP/GaAs double junction solar cells continues to improve with the optimized material quality and device processing [2].

The GaInP single junction solar cells (SJSC), proposed by T. Takamoto in 1994, show an efficiency (η) of 17.4% using metalorganic chemical vapor deposition method with emitter and base thicknesses of 0.05 µm and 1.5 µm respectively [3]. In 1997, Ming-Ju Yang fabricated a GaInP SJSC on a GaAs and Si substrates by MOCVD that gives a record efficiency of 18.5% at AM I.5 with total thickness device of 2.38 µm [4]. J.W. Leem obtained a conversion of 13.34% with a 0.91 µm thickness solar cell by optimizing the base thickness of the top GaInP cell in 2009[5]. In 2011, Shulong Lu achieved an efficiency of 16.4% at single concentration of one sun and air mass 1.5 global by using an AlInP as the window layer, GaInP as the back surface field (BSF) layer, and GaAs as the buffer layer and with a total cell thickness of 0.93 µm. The Lu's cell was designed using all solid-state molecular-beam-epitaxy (MBE) technique [2]. In another study, conducted by J. F. Geisz *et al* 2013, an efficiency of 20.08% was achieved for GaInP rear

---

heterojunction grown by atmospheric-pressure metalorganic vapor phase epitaxy (MOVPE) with a total thickness of 1μm [6]. In 2015, P.P. Nayak an efficiency of 21.85% at one sun and AM1.5 global is attained by using an AlGaInP as the double BSF layer with a total cell thickness of 0.68 μm for top cell [7]. In the paper presented by Ahmed Benlekhdim 2018, an efficiency of 18.55% was reported by optimizing the AlGaAs of both the layers of the window and the buffer; and the GaInP BSF layer with a solar cell thickness of 0.86 μm [8]. Moreover, in 2018, Kuan W.A. Chee optimized the thickness and doping of the base layer and then compared the Single Junction solar cells to the double junction solar cells in terms of their efficiency. Their study showed that the efficiency of the top cell (GaInP) under AM.0 illumination of 17.89% with a device thickness of 0.66 μm [9].

Recently, Martin A. Green *et al*. from the National Renewable Energy Laboratory (NREL) have demonstrated a high efficiency 22.00% for a GaInP solar cell measured under the global AM1.5 spectrum (1000 W/m^2) at 25°C [10]. Also, in 2020, M. Benaicha used a GaInP layer as a top cell in a GaInP/Si multi-junction monolithic solar cell, with a cell thickness of 1.07 μm, which demonstrates an efficiency of 20.99% [11]. In addition, Manish Verma has obtained an efficiency of 21.59% for GaInP SJSC with a double layer BSF at AM1.5G spectrum and with a structure having a thickness of 0.725 μm [12].

In this paper, we present a design of GaInP SJSC that improves the cell efficiency through the optimization of current matching between n-base and p-emitter layers. This is carried out by varying the thicknesses of both layers and with the optimization of the doping and thicknesses of the AlGaAs buffer and the AlGaInP window layers. The conversion efficiency and the external quantum efficiency (*EQE*) are investigated for different n-base/p-emitter layers thicknesses. The proposed optimization approach is based on the simulation of the solar cell under 1 sun and AM1.5G spectrum at room temperature of 25°C. The obtained results, using Atlas tool of SILVACO TCAD, are compared to the previously reported simulation and experimental results.

2. Theoretical analysis

2.1. Device Structure

The designed solar cell is based on an GaInP PN junction with AlGaInP (p+) doped window, AlGaInP (n+) doped BSF and AlGaAs buffer (n+) doped. The energy bandgaps for the GaInP and AlGaAs at room temperature are calculated using formulas provided in [13,14]:

$$E_g\left(GaInP\right) = 1.35 + 0.73x + 0.7x^2 \left[eV\right] \tag{1}$$

$$E_g\left(AlGaAs\right) = 1.9 + 0.125x + 0.143x^2 \left[eV\right] \tag{2}$$

Using these formulas, the energy bandgaps for $Ga_{0.51}In_{0.49}P$ and $Al_{0.7}Ga_{0.3}As$ are: 1.9 eV and 2.06 eV respectively.

The Atlas simulation results of the solar cell structure with the thicknesses and the doping concentration of all the layers is presented in Figure 1 and summarized in table 1.
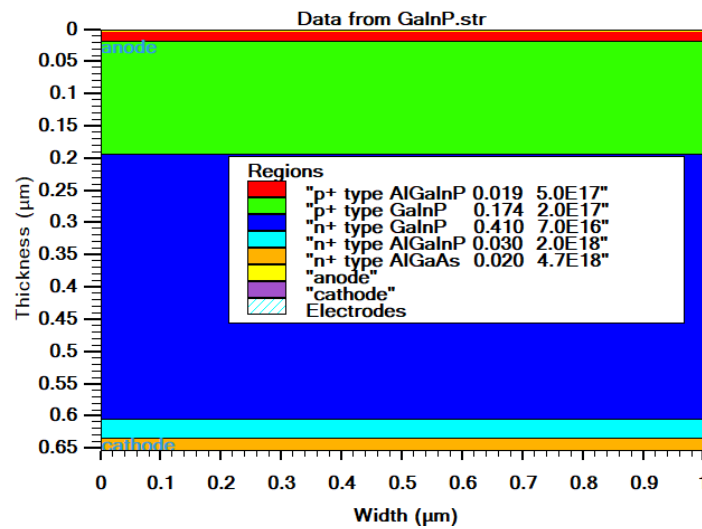
Fig. 1. Optimized Structure of GaInP SJSC.

Table. 1 Thicknesses and doping concentrations of the layers of the simulated structure.

Layer	Material	Doping type	Thickness (μm)	Concentration (cm^{-3})
Window	$(Al_{0.7}Ga_{0.3})_{0.5}In_{0.5}P$	P	0.019	5.0×10^{17}
Emitter	$Ga_{0.51}In_{0.49}P$	P	0.174	2.0×10^{17}
Base	$Ga_{0.51}In_{0.49}P$	N	0.410	7.0×10^{16} [15]
Back Surface Field	$(Al_{0.7}Ga_{0.3})_{0.5}In_{0.5}P$	N	0.030 [16]	2.0×10^{18} [15]
Buffer	$Al_{0.7}Ga_{0.3}As$	N	0.020	4.7×10^{18}

2.2. Material Properties for different Layers

The main optical properties of a semiconductor material are the refractive index and the absorption coefficient. These properties are very important for optoelectronic components since they govern the movement of light in the component. For example, in a component made of different materials, the light tends to propagate in the materials with the highest refractive index.

The basic optical input parameters for Atlas-Silvaco simulation for each material are the refractive index n(λ) and extinction coefficient k(λ) [17]. These parameters are defined by using Adachi's model for GaInP and AlGaAs compound materials as highlighted in Figures 2 and 3 [18-20]:
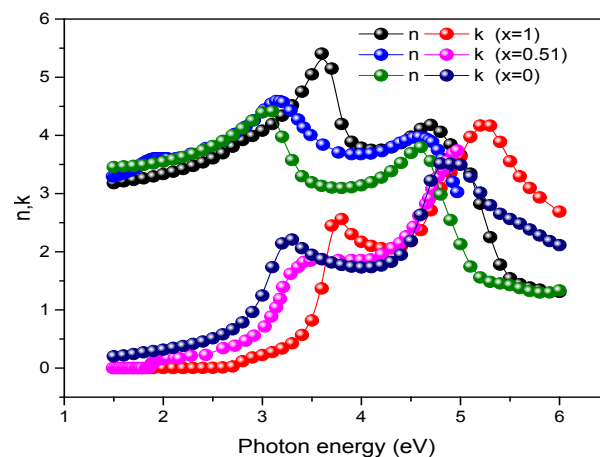

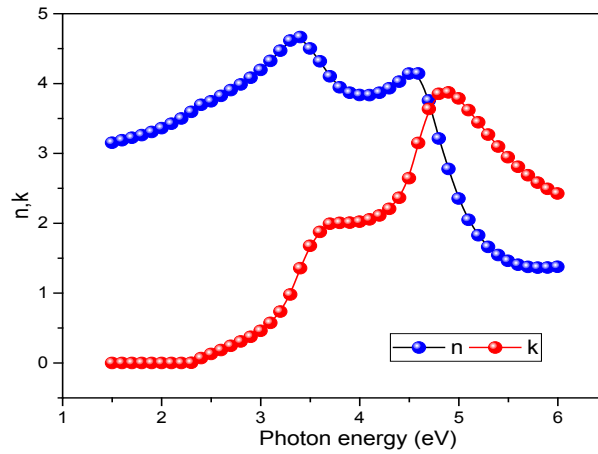*Fig. 2. Refractive index (n) and extinction coefficient (k) versus photon energy of $Ga_xIn_{1-x}P$.*

Fig. 3. Refractive index (n) and extinction coefficient (k) versus photon energy of Al$_{0.7}$Ga$_{0.3}$As

The parameters of each layer of the ternary materials Ga$_{0.51}$In$_{0.49}$P, Al$_{0.7}$Ga$_{0.3}$As and quaternary (Al$_{0.7}$Ga$_{0.3}$)$_{0.5}$In$_{0.5}$P used in this structure are presented in Table 2 [14,17, 19,21, 22,23]:

Table. 2 Parameters of the materials used in this design.

Material	GaInP	AlGaInP	AlGaAs
Band gap E$_g$[eV] at 300K	1.90	2.33	2.06
Lattice constant [Å]	5.65	5.65	5.66
Relative dielectric permittivity	11.79	11.70	11.2
Electron Affinity [eV]	4.08	4.20	3.54
Heavy e– effective mass [me*/m0]	3	2.85	2.40
Heavy h+ effective mass [mh*/m0]	0.64	0.64	0.755
e– mobility MUN [cm^2/(V×s)]	1945	2150	2000
h+ mobility MUP [cm^2/(V×s)]	141	141	138
n$_{ie}$ (p$_{er\ cc}$)	7.4×10^4	1	1.37×10^3
v$_{satn}$ (cm/s)	1.0×10^6	1.0x10^6	7.70×10^6
v$_{satp}$ (cm/s)	1.0×10^6	1.0x10^6	7.70×10^6

2.3. Physical Models

Among the numerous mechanisms of generation-recombination used to simulate solar cells in Atlas tool of SILVACO TCAD, the Shockley-Hall-Read is the most useful. The SRH model provides the best results which are close to the experimental results [23]. In the present work, Shockley-Read-Hall recombination (SRH) model is used to simulate the recombination effects that occur inside the various part of the device surface. The SRH model used in this work is given by [17,24]:

$$R_{SRK} = \frac{(pn - n_{ie}^2)}{v_p\left[n + n_{ie}e^{\left(\frac{E_{trap}}{KT_L}\right)}\right] + v_n\left[n + n_{ie}e^{\left(\frac{-E_{trap}}{KT_L}\right)}\right]} \quad (3)$$

$$v_{n(p)} = v_{n(p)0}\left(\frac{1+N}{N_{SRKN(P)}}\right) \quad (4)$$

where $p(n)$ is the number of electrons (holes), n_{ie} is the intrinsic carrier concentration, E_{trap} is the difference between the trap energy level and the intrinsic Fermi level, T_L is the lattice temperature in Kelvin, $v_{n(p)}$ is the electron (hole) lifetime, N is the total impurity concentration, $N_{SRKN(P)}$ is a

constant which determines the concentration from which the electron (hole) lifetime start to deteriorate.

2.4. Solar cell characteristic parameters

The main parameters of the solar cell are the J_{sc}, V_{oc}, FF, η, and the total external quantum efficiency (EQE_{tot}). The EQE or spectral response (SR) is the standard function that provide the information about the generation and recombination physical phenomena of the solar cell [24].

The EQE_{tot} of an ideal cell with a total thickness (w) of the three regions of the PN junction composing the structure is defined by the sum of the $EQEs$, that is, (EQE_{Base}, $EQE_{emitter}$ and $EQE_{depletion}$) as given by the standard equations [25,26].

$$EQE_{tot} = EQE_{emitter} + EQE_{depletion} + EQE_{base}e^{-\alpha(d_e+w)} \tag{5}$$

$$EQE_{emitter} = \frac{\alpha L_e}{(\alpha L_e)^2-1}\left[\frac{\ell l_e+\alpha L_e-e^{(-\alpha d_e)}\times[l_e\cos\Box(\beta_e)+\sin\Box(\beta_e)]}{\cos\Box(\beta_e)+l_e\sin\Box\beta_e} - \alpha L_e e^{(-\alpha d_e)}\right] \tag{6}$$

$$EQE_{depletion} = \left[1 - e^{(-\alpha w)}\right]e^{(-\alpha d_e)} \tag{7}$$

$$EQE_{base} = \frac{\alpha L_b}{(\alpha L_b)^2-1}\left[-\frac{\ell(\alpha L_b-l_b)e^{(-\alpha d_b)}+l_b\cos\Box(\beta_b)+\sin\Box(\beta_b)}{\cos\Box(\beta_b)+l_b\sin\Box(\beta_b)} + \alpha L_b\right] \tag{8}$$

$$\beta_e = \frac{d_e}{L_e}, \quad \beta_b = \frac{d_b}{L_b}, \quad l_b = \frac{qS_bL_b}{kT\mu_b} \quad and \quad l_e = \frac{qS_eL_e}{kT\mu_e} \tag{9}$$

The quantities $\mu_{b(e)}$, $L_{b(e)}$, and $S_{b(e)}$ are, respectively, the mobility, diffusion length, and surface recombination velocity for the minority carriers in the base(emitter), and T is the absolute temperature, and d_e, d_b, and w are thicknesses of base, emitter and depletion layers respectively.

The relation that gives the dependance of EQE_{tot} to the total thickness of the device $d=d_e+w+d_b$ is as follows:

$$EQE_{tot}(\lambda) = 1 - e^{-\alpha(\lambda)d} \tag{10}$$

The J_{sc} is determined by the EQE and by the flux of the spectrum photon (ϕ_{inc}) at AM1.5G as shown by the following expression [25]:

$$J_{sc} = q\int_{\lambda_1}^{\lambda_2} EQE_{tot}(\lambda)\phi_{inc}^{AM1.5}(\lambda)d\lambda \tag{11}$$

where q is the elementary electron charge, λ_1 is the cutoff wavelength of the solar spectrum and λ_2 is the GaInP cutoff wavelength determined by the absorption coefficient α, and it is approximately equal to hc/E_g, where E_g is the energy gap of GaInP [27].

The V_{oc} and FF are calculated using the following relations [28]:

$$V_{oc} = \frac{nKT}{q}ln\left(\frac{J_L}{J_0} + 1\right) \tag{12}$$

$$FF = \frac{J_{max}V_{max}}{J_{sc}V_{oc}} \tag{13}$$

where,

K is Boltzmann's constant;
J_L is the light generated current density;
T is the temperature;
n is the ideality factor;
J_0 is the saturation current density.

The efficiency of the solar cell is given by the ratio of the available maximum power (P_{max}) to the incident power of AM1.5G spectrum (P_{inc}) that obtained through the following equation [29]:

$$\eta = \frac{P_{max}}{P_{inc}} \frac{(V_{oc}J_{sc}FF)}{P_{inc}} \tag{5}$$

3. Simulation results and discussions

The optimization of the n-base/p-emitter was carried out by finding the layer thicknesses that maximize the J_{sc} of the solar cell. The investigated thickness range, (L_P, L_N), is 0,05 to 0,30 µm for the n-base and 0,10 to 0,70 µm for the p-emitter. The obtained corresponding diagram band energy of the GaInP cell is presented in Fig.4. And the corresponding J_{sc} as a function of the n-base thickness for different thickness values of the p-emitter layer is presented in Fig. 5.
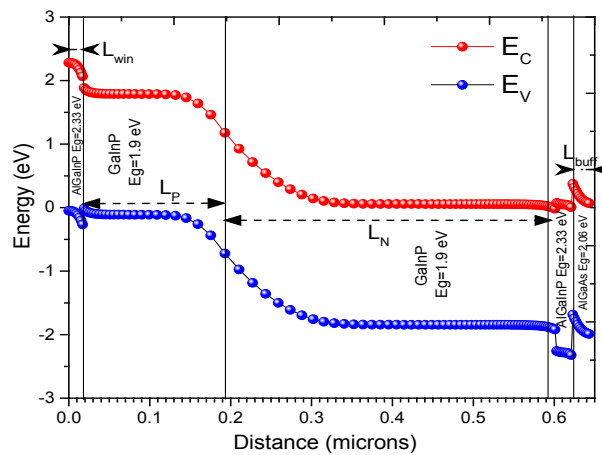

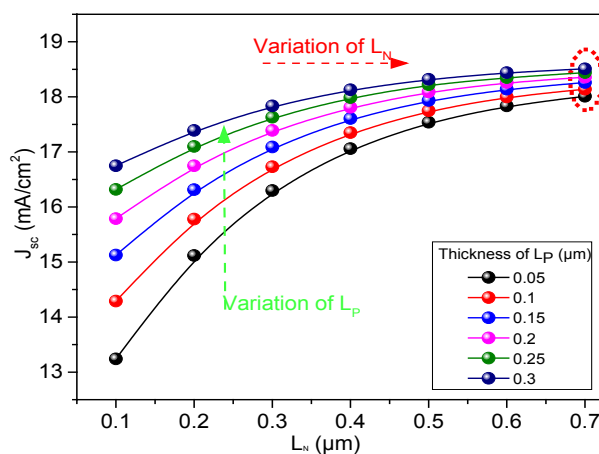*Fig. 4. Schematic energy band diagram of the GaInP SJSC.*

Fig. 5. Short-circuit current density as a function of the n-base thickness (L_N) for p-emitter various thickness (L_P).

Figure 5 shows the variation of the cell short-circuit current density in term of both the thicknesses of the n-base and the p-emitter layers. This variation shows that there is more

absorption of optical photons, which leads to a higher short current, with the increase of the both L_N and L_P. This J_{sc} saturates when it reaches 18.30 mA/cm^2 which corresponds to 0.70 μm of n-base thickness. At this level the J_{sc} is independent of p-emitter thickness.

Figure 6 presents the variation of the voltage open circuit (V_{oc}) as function of both the thicknesses of the n-base and the p-emitter layers. It shows a slight variation (decrease) with the increase of the thickness of the p-emitter layer (L_P). Therefore, the V_{oc} it is relatively independent of the p-emitter layer thickness (L_N).
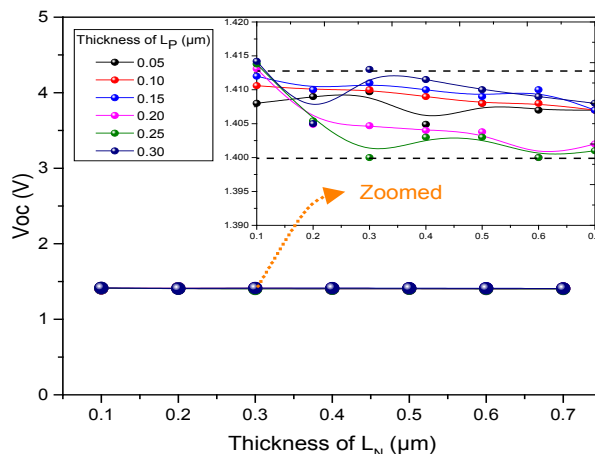

Fig. 6. Open-circuit voltage as a function of the n-base thickness (L_N) for various p-emitter thickness (L_P).

The fill factor (FF), which describes the quality of a solar cell, is shown in Fig. 7. The FF demonstrates a big dependence on thickness of the n-base layer. This can be explained by the variation of the bulk resistance of the absorber layer, which depends on the thickness of the n-base layer.
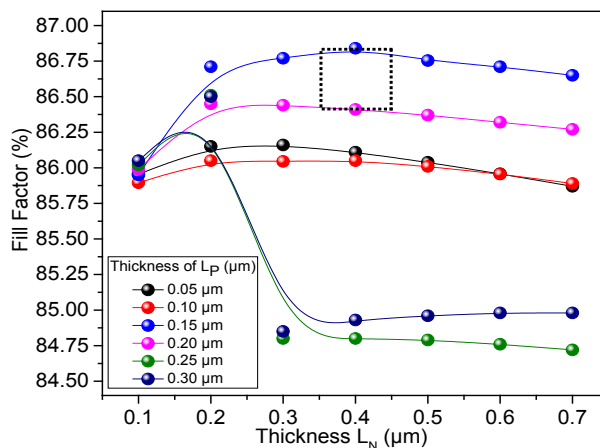

Fig. 7. Fill Factor as a function of the n-base thickness (L_N) for various p-emitter thickness (L_P).

According to these results, the best value of the FF falls in the regions delimited by the thickness interval {0.15-0.20} of the p-emitter layer and the thickness interval {0.35-0.45} of the n-base layer. Additionally, as shown in Fig. 7, when L_P and L_N increase, the FF decreases.

The results shown in Fig.8 are the variations of the EQE with respect to wavelength for different thickness of the n-base and the p-emitter layers. The optimum value of EQE is 0.688 for the GaInP cell. This value is achieved with the thicknesses of 0.410 μm and 0.175 μm of the n-base and p-emitter layers respectively. The optimized value of the EQE is obtained in the

wavelength range of 550 nm. This result is very significant if compared to that reported in the literature, an optimum value of EQE for the top cell of 0.672 [30].

According to eq. 10, since the EQE depends on the thicknesses of both p-emitter and n-base layers, it can be improved by optimizing these thicknesses.
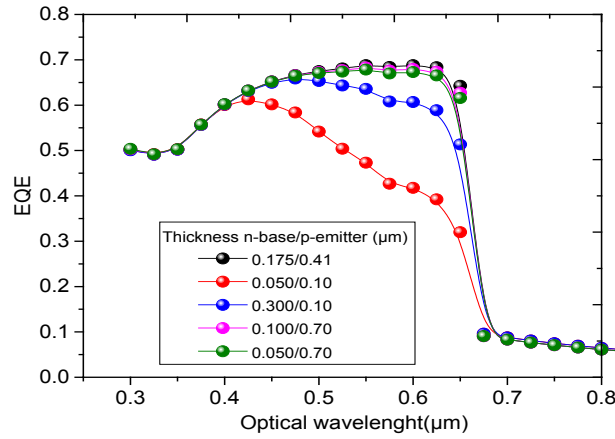

Fig. 8. External quantum efficiencies as a function of wavelength for various L_P/L_N thicknesses under AM1.5 illumination.

The Variations of both thicknesses of the base and emitter layers affect the properties of the solar cell as shown in Figures 5, 6 and 8. In addition, reducing the recombination rate in the P/N layers can improve the solar cell efficiency. This reduction can be done by reducing the junction area. Figure 9 shows the efficiency of the GaInP solar cell as a function of the simultaneous variation of the n-base and p-emitter thicknesses. From this result, we can extract the two thicknesses L_N and L_P that can lead to the optimal energy conversion of the solar cell. Accordingly, the optimal conversion is obtained for L_N and L_P of 0.410 µm and 0.174 µm respectively.
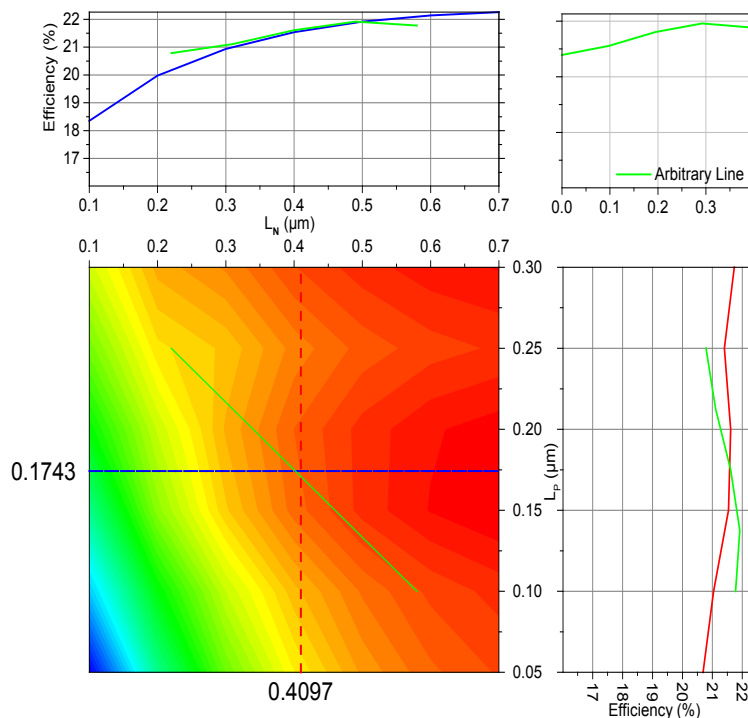

Fig. 9. Efficiency of GaInP solar cell as a function of n-Base/p-Emitter thicknesses.

The window and the buffer layers play an important role to minimize the dispersion of the carriers so that the charge carriers accumulate near these window and buffer layers, therefore increasing the rate of photogeneration [31]. Additionally, the presence of the AlGaAs buffer causes a relative increase in J_{sc}, FF and η due to the reduction of the recombination rate in this area. The maximum value of the efficiency is attained by optimizing the thicknesses (L_{win}, L_{buff}) and the doping concentration (N_{win}, P_{buff}) of the window and the buffer layer. Figures 10 and 11 present the diagrams of the efficiency of the proposed solar cell as a function of two parameters - doping and thickness of the window and buffer layers. The optimal values of (L_{win}, N_{win}) and (L_{buff}, P_{buff}) which corresponds to the maximum efficiency are: (L_{win}=0.019 μm, N_{win} = 5.019×10^{18} cm^{-3}) and (L_{buff}=0.020 μm, P_{buff}=4.754×10^{18} cm^{-3}).
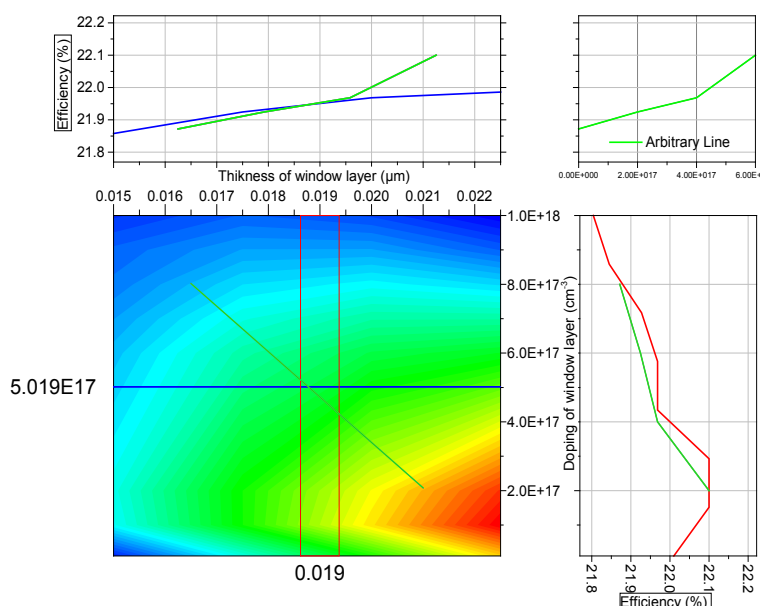

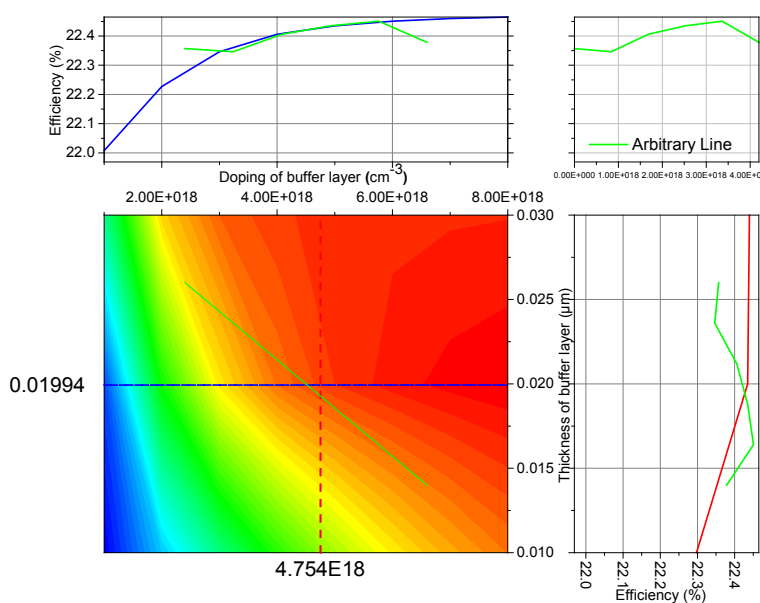Fig. 10. *Efficiency of GaInP solar cell as a function of window thickness and doping.*

Fig. 11. *Efficiency of GaInP solar cell as a function of buffer thickness and doping.*

The current voltage (J-V) and power voltage (P-V) characteristics of the solar cell, corresponding to the optimized parameters, are depicted in Fig.12. From these characteristics, it can be concluded that the thickness of the n-base/p-emitter layers has a significant effect on the shape of the J-V characteristic of the GaInP solar cell with AlGaAs as a buffer and AlGaInP as both BSF and window layers.
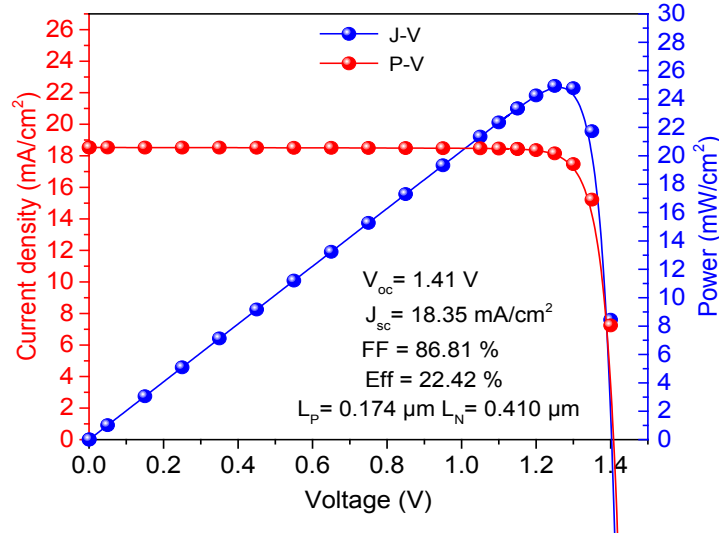

Fig. 12. J-V and P-V curves of the optimized single junction solar cell.

Table 3 gives the different characteristics and parameters of the simulated solar cell and the single junction GaInP solar cells reported in the literature. The comparison of these results brings out that the optimal P/N thicknesses is obtained when an AlGaAs buffer layer is added to the GaInP solar cell. Consequently, this improves the efficiency conversion of the solar cell and helps to reduce the total thickness of the solar cell which reduces the cost of the solar cell. It can also be used to improve the absorbance of the bottom solar cell for a dual-junction solar cell, this subject will be explored in future studies.

Table. 3 Comparison of the important parameters in the proposed design and the published designs under AM1.5 illumination.

Description [Ref]	cell thickness (μm)	J_{sc} (mA/cm^2)	V_{oc} (V)	FF (%)	η (%)
GaInP SJSC [3]	2.380	28.79	1,39	86.90	17.40
GaInP SJSC [4]	2.380	15.12	1.39	87.90	18.49
GaInP SJSC [5]	0.910	10.60	1.26	85.25	13.34
GaInP SJSC [2]	0.930	13.50	1.37	88.00	16.40
GaInP SJSC [6]	1.000	16.00	1.46	89.30	20.80
GaInP SJSC [7]	0.680	16.79	1.50	90.25	21.85
GaInP SJSC [8]	0.860	14.80	1.41	88.67	18.55
GaInP SJSC [9]	-	16.63	1.47	90.20	22.00
GaInP SJSC [10]	1.070	16.75	1.45	86.11	20.99
GaInP SJSC [11]	0.725	18.33	1.44	85.60	21.59
GaInP [our work]	0.650	18.35	1.41	86.81	22.42

4. Conclusion

In this work, the design and simulation of an GaInP single junction solar cell was carried out using Atlas tool of SILVACO TCAD. The solar cell was optimized by varying both thicknesses of the n-base layer and the p-emitter layer of the GaInP solar cell and by adjusting the window thickness and doping level. Also, by adding the AlGaAs buffer layer to basic solar cell structure. The test performance parameters of the optimized solar cell are an efficiency (η) of 22.42%, a short circuit current density (J_{sc}) equal to 18.35 mA/cm^2, an open circuit voltage (V_{oc}) equal to 1.41V and a fill factor (FF) equal to 86.81%.

These optimal values were obtained using 0,410 μm and 0,174 μm for n-base layer (L_N) and p-emitter layer (L_P) respectively and the thicknesses (L_{win}, L_{buff}) and doping concentrates (N_{win}, P_{buff}) of the window and the buffer layers: (L_{win}=0.019 μm, N_{win} = 5.019×10^{17} cm^{-3}) and (L_{buff} =0.020 μm, P_{buff} =4.754×10^{18} cm^{-3}). From the solar cell simulation results, it follows that the reduction of thickness of the solar cell is about of 0.65 μm, which is smaller than what is reported in the listed literature studies.

Acknowledgements

References

[1] E. Ochoa-Martínez, L. Barrutia, M. Ochoa, E. Barrigón, E. Garcia, I. Rey-Stolle, M. Gabás, Solar Energy Materials and solar cells, 174, 388(2018); https://doi.org/10.1016/j.solmat.2017.09.028

[2] S. Lu, L. Ji, W. He, P. Dai, H. Yang, M. Arimochi, M. Ikeda, Nanoscale research letters, 6(1), 1(2011); https://doi.org/10.1186/1556-276X-6-576

[3] T. Takamoto, E. Ikeda, H. Kurita, M. Ohmori, Solar energy materials and solar cells, 35, 25(1994); https://doi.org/10.1016/0927-0248(94)90118-X

[4] M. J. Yang, M. Yamaguchi, T. Takamoto, E. Ikeda, H. Kurita, M. Ohmori, Solar Energy Materials and Solar Cells, 45(4), 331(1997); https://doi.org/10.1016/S0927-0248(96)00079-7

[5] J. W. Leem, Y. T. Lee, J. S. Yu, Optical and quantum electronics, 41(8), 605(2009); https://doi.org/10.1007/s11082-010-9367-1

[6] J. F. Geisz, M. A. Steiner, I. Garcia, S. R. Kurtz, D. J. Friedman, Applied Physics Letters, 103(4), 041118(2013); https://doi.org/10.1063/1.4816837

[7] P. P. Nayak, J. P. Dutta, G. P. Mishra, Engineering Science and Technology, an International Journal, 18(3), 325(2015); https://doi.org/10.1016/j.jestch.2015.01.004

[8] A. Benlekhdim, A. Cheknane, L. Sfaxi, H. S. Hilal, Optik, 163, 8(2018); https://doi.org/10.1016/j.ijleo.2018.02.113

[9] K. W. Chee, Y. Hu, Superlattices and Microstructures, 119, 25(2018); https://doi.org/10.1016/j.spmi.2018.03.071

[10] M. A. Green, E. D. Dunlop, J. Hohl-Ebinger, M. Yoshita, N. Kopidakis, X. Hao, solar cell efficiency tables (version 56), Progress in Photovoltaics: Research and Applications, 28(7), 629(2020); https://doi.org/10.1002/pip.3303

[11] M. Benaicha, L. Dehimi, F. Pezzimenti, F. Bouzid, Journal of Semiconductors, 41(3), 032701(2020); https://doi.org/10.1088/1674-4926/41/3/032701

[12] M. Verma, S. R. Routray, G. P. Mishra, Materials Today: Proceedings, 43, 3420(2021);

1202

https://doi.org/10.1016/j.matpr.2020.09.073

[13] G. B. Stringfellow, Journal of Applied Physics, 43(8), 3455(1972; https://doi.org/10.1063/1.1661737

[14] S. Adachi, Journal of Applied Physics, 58(3), R1-R29(1985); https://doi.org/10.1063/1.336070

[15] J. P. Dutta, P. P. Nayak, G. P. Mishra, Optik, 127(8), 4156(2016); https://doi.org/10.1016/j.ijleo.2016.01.041

[16] K. J. Singh, N. B. Singh, S. K. Sarkar, Journal of Computational Electronics, 14(1), 288(2015); https://doi.org/10.1007/s10825-014-0652-2

[17] ATLAS Device Simulation Software User's Manual, Silvaco International, Santa Clara, CA, 2013.

[18] D. E. Aspnes, A. A. Studna, Physical review B, 27(2), 985(1983); https://doi.org/10.1103/PhysRevB.27.985

[19] M. Schubert, V. Gottschalch, C. M. Herzinger, H. Yao, P. G. Snyder, J. A. Woollam, Journal of Applied Physics, 77(7), 3416(1995); https://doi.org/10.1063/1.358632

[20] O. J. Glembocki, K. Takarabe, Aluminum gallium arsenide ($Al_xGa_{1-x}As$). Handbook of Optical Constants of Solids. Academic Press, 513(1997); https://doi.org/10.1016/B978-012544415-6.50066-2

[21] Y. A. Goldberg, Gallium indium phosphide ($Ga_xIn_{1-x}P$), Handbook Series on Semiconductor Parameters: Volume 2: Ternary and Quaternary III-V Compounds, 37-61 (1996); https://doi.org/10.1142/9789812832085_0002

[22] Y. A. Goldberg, Aluminium gallium arsenide ($Al_xGa_{1-x}As$), Handbook Series on Semiconductor Parameters: Volume 2: Ternary and Quaternary III-V Compounds, 43(F43m),1-36(1996); https://doi.org/10.1142/9789812832085_0001

[23] K. J. Singh, S. K. Sarkar, Optical and Quantum Electronics, 43(1), 1(2012); https://doi.org/10.1007/s11082-011-9499-y

[24] D. S. Ginley, D. (Eds.). Cahen, Fundamentals of materials for energy and environmental sustainability, Cambridge University press, (2011); https://doi.org/10.1017/CBO9780511718786

[25] J.M. Olson, D.J. Friedman, S. Kurtz, High-efficiency III-V multijunction solar cells, In: Luque, A., Hegedus, S. (eds.) Handbook of Photovoltaic Science and Engineering, John Wiley & Sons, pp. 359-411(2003); https://doi.org/10.1002/0470014008.ch9

[26] H. J. Hovel, "Semiconductors and semimetals". Volume 11. Solar cells, United States, (1975); https://doi.org/10.1063/1.3024511

[27] C. T. Sah, P. C. H. Chan, C. K. Wang, R. Y. Sah, K. A. Yamakawa, R. Lutwack, IEEE Trans. Electron Devices, 28(3), 304(1981); https://doi.org/10.1109/T-ED.1981.20333

[28] B. Farhadi, M. Naseri, Optik, 127(15), 6224(2016); https://doi.org/10.1016/j.ijleo.2016.04.039

[29] H. Mathieu, H. Fanet, Physique des semiconducteurs et des composants électroniques - 6ème édition, Dunod, Paris, (2009).

[30] J. Verma, P. Dey, A. Prajapati, T. D. Das, Multi BSF Layer GaInP/GaAs High Efficiency Solar Cell, In. Proc, ISOC 2017, 11th International Conference on Intelligent Systems and Control, National Institute of Technology, Arunachal Pradesh, India (2017); https://doi.org/10.1109/ISCO.2017.7855998

[31] H. R. Arzbin, A., Materials Science and Engineering: B, 243, 108 (2019); https://doi.org/10.1016/j.mseb.2019.04.001